

The tensile properties of pultruded GRP tested under superposed hydrostatic pressure

T. V. PARRY*, A. S. WRONSKI

Engineering Materials Research Group, University of Bradford, Bradford, West Yorkshire BD7 1DP, UK

The failure mechanisms in waisted tensile specimens of pultruded 60% volume fraction glass fibre-epoxide were investigated at atmospheric and superposed hydrostatic pressures extending to 350 MN m^{-2} . The maximum principal stress at fracture decreased from $\sim 1.7 \text{ GN m}^{-2}$ at atmospheric pressure to $\sim 1.3 \text{ GN m}^{-2}$ at 250 MN m^{-2} superposed pressure and remained approximately constant at higher pressures, as had been observed with carbon fibre reinforced plastic (CFRP) and a nickel-matrix carbon fibre composite. In the high-pressure region the failure surfaces were fairly flat, consistent with the fracture process being solely controlled by fibre strength. Pre-failure damage, in particular debonding, was initiated at $\sim 0.95 \text{ GN m}^{-2}$ at atmospheric pressure and this stress rose to $\sim 1.2 \text{ GN m}^{-2}$ at 300 MN m^{-2} superposed pressure, i.e. by about 9% per 100 MN m^{-2} . Unlike the pressure dependence in CFRP, this contrasts with the pressure dependence of the resin tensile strength, about 25% per 100 MN m^{-2} , but can be associated with that of the fibre bundle/resin debonding stress, about 12% per 100 MN m^{-2} superposed pressure. Consistent with this interpretation, glass fibres of the failure surfaces were resin-free, again in contrast to CFRP.

1. Introduction

Theories of the tensile strength of high volume fraction, V_f , of unidirectionally-aligned fibrous composites relate it to the breaking strength of the fibres [1-6]. Interestingly the experiments often cited to support detailed microstructural models are those of Rosen [6] on a 6% V_f glass fibre reinforced plastic (GRP) lamina of about 100 fibres in total. Fibres in a well-chosen matrix are postulated to reach their breaking strain before matrix failure, reducing its role to the isolation of fibre breaks into a narrow section.

Microstructural studies of carbon fibre reinforced plastic (CFRP) and GRP specimens strained to and below their failure strengths in tension, compression and bending, particularly under superposed hydrostatic pressure, have enabled us [7-11] to re-examine the problem and draw attention to the role of detachment and delamination of surface fibre bundles in failure mechanisms. In particular we have suggested that, as in CFRP this delamination is controlled by the strength of the resin matrix, similarities in the axial tensile and compressive behaviour of CFRP can be accounted for without recourse to hypotheses involving shear-stress [12] controlled failure of carbon fibres in tension and compression.

The tensile properties of glass are even less likely to be controlled by shear stresses, glass being *the* Griffith material. Accordingly it was decided to study also GRP in tension under superposed hydrostatic pressure, H . We would recall that such a stressing environment enables discrimination between shear stress-operated mechanisms (unaffected by H) and tensile

stress-operated mechanisms (directly affected by H). Of fibrous composites studied by us only in a 56% V_f carbon fibre-nickel composite did the maximum principal tensile stress for failure remain constant as H varied; in CFRP it decreased with H till 200 MN m^{-2} pressure and only at higher pressures was it constant.

2. Experimental procedure

Specimens were machined from 6 mm diameter pultruded rods supplied by AERE, Harwell. They contained $\sim 60\%$ V_f of S glass fibres in an epoxy resin matrix. The majority of the specimens tested were of the design illustrated in Fig. 1a of our previous paper [8] and contained no gauge length of constant cross-section. The section was reduced, over a length of 10 mm and with a radius of 12.5 mm, to a minimum diameter of 0.8 to 1.0 mm. This ensured tensile failures whilst using the maximum shoulder length (~ 30 mm) that could be accommodated within the limited space available inside the pressure cell. Some samples were unloaded before failure for microscopic examination.

All specimens were strained in uniaxial tension on a Hedeby universal tester at a rate of 0.1 mm min^{-1} . The machine was fitted with a Coleraine pressure cell which allowed the superposition of pressure extending to 350 MN m^{-2} using Plexol, a synthetic diester, as a medium. Experimental details have been presented in our previous papers [7-9, 11]. The failure surfaces and adjoining surface areas of some specimens were examined on an ISI Super III scanning electron microscope. Other samples were mounted in polyester resin and sectioned and polished parallel to the fibre

*Present address: Applied Mechanics Group, School of Engineering and Applied Sciences, University of Durham, UK.

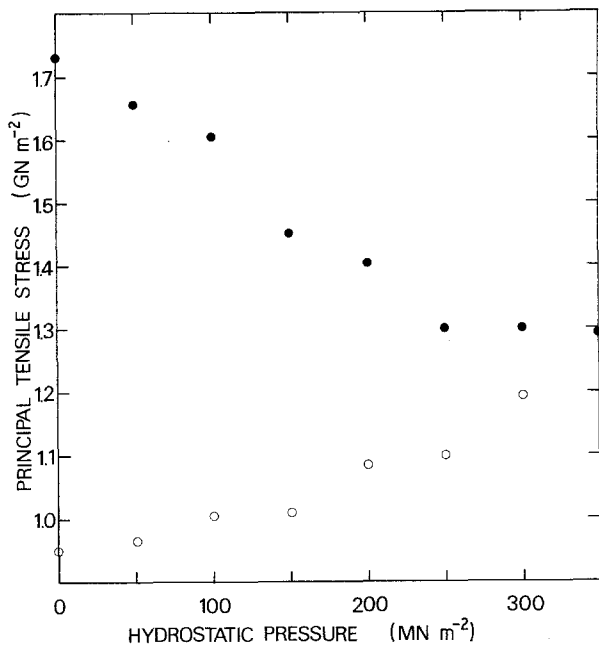


Figure 1 Maximum principal stresses (○) at the limit of proportionality, and (●) at failure, for GRP tensile specimens tested under superposed hydrostatic pressure.

axis prior to examination on the SEM or a Zeiss Ultraphot II optical microscope. To delineate clearly the transverse cracks emanating from the minimum cross-section of deformed specimens, a "dye penetrant/cellulose paint" technique, developed for CFRP [10] was employed. It enabled length measurements of the "tramline" cracks in the shoulders and heads of the tensile specimens.

3. Results

The atmospheric tensile strength of our GRP material was $\sim 1.7 \text{ GN m}^{-2}$, and this (the maximum principal tensile stress) decreased, approximately linearly, to $\sim 1.3 \text{ GN m}^{-2}$ when $H = 250 \text{ MN m}^{-2}$ was applied (Fig. 1). It remained approximately constant as H was raised to 350 MN m^{-2} , the limit of our apparatus. The load-deflection curves indicated deviations from linearity prior to failure at all pressures except the highest. The critical stress for this rose from $\sim 0.95 \text{ GN m}^{-2}$ at atmospheric pressure, to $\sim 1.2 \text{ GN m}^{-2}$ at 300 MN m^{-2} superposed pressure (Fig. 1).

Concurrently at these and higher levels of tensile stress, damage was observed on the surfaces of strained specimens. Examples, for failed specimens, at atmospheric, 100, 200, 300, and 350 MN m^{-2} superposed pressures are presented in Figs 2 and 3. It is seen that inter-tow cracks had formed and appear to be associated with the minimum cross-section. This cracking was further investigated by preparing longitudinal sections, and the delaminations were seen to follow resin-rich areas between tows which make up the pultrusion. Their lengths decreased (Table I) from $\sim 20 \text{ mm}$ (but not systematically, as in CFRP [10]), with increasing pressure; no "tramlines" were detected in the specimen tested at 350 MN m^{-2} . In a similar way to CFRP, the fracture topography altered from "random bundle" [10] at atmospheric pressure to a localized failure at the minimum cross-section but was

TABLE I The variation with superposed pressure in the length that transverse cracks grow to before tensile failure of pultruded GRP

Superposed pressure (MN m ⁻²)	Crack length (mm, $\pm 2 \text{ mm}$)
Atmospheric	20
50	23
100	22
150	18
200	12
250	9
300	5
350	0

still associated, in contrast to CFRP, with some inter-laminar cracking (Figs 2 and 3). To note also is the "clean" appearance of the glass fibres in the failed bundles, in marked contrast to carbon fibres which had epoxide resin adhering to them (Fig. 4).

4. Discussion

The general features of these GRP data resembled somewhat the results of a similar study of CFRP [10]. In interpreting that work we postulated a three-stage failure process: debonding of surface bundles (dependent on specimen geometry) associated with straightening of surface fibre bundles against the transverse support to the matrix, delamination or growth of the inter-tow cracks to detach the surface bundles such that they are unable to carry tensile load and finally, when a critical stress has been transferred to the remaining fibre bundles, catastrophic failure.

In CFRP the critical stress for delamination was associated with resin yielding, as the fibre/matrix interface was not broken. The pressure dependence of this stress corresponded well with that of the epoxide resin yield stress ~ 0.25 per 100 MN m^{-2} superposed pressure [10, 13]. In the GRP currently studied this is substantially lower, ~ 0.09 per 100 MN m^{-2} pressure, and the fibre surfaces are exposed by failure. It is therefore suggested that the critical tensile stress for debonding of surface bundles is

$$\sigma_c = \frac{4R\sigma_a}{\pi D} \quad (1)$$

where R is the existing radius of curvature of a fibre bundle of diameter D , and σ_a is the stress for interfacial decohesion. This relation substitutes σ_a for σ_t , the matrix tensile strength, in the relation presented in our previous paper [10], and also halves it, consistent with the relevant bundles being in the surface and in accord with the details of our analysis [10, 14, 15] rather than Piggott's [16] development of Swift's [17] model for compressive strength.

The interfacial properties of glass/resins have been recently investigated by Chua and Piggott [18, 19], who found for epoxide maximum interfacial shear stresses of 21 to 34 MN m^{-2} . They extended their studies to consider transverse compression [20, 21] and concluded that the value of interfacial pressure, P , resulting from cure shrinkage for single fibres was 18 to 26 MN m^{-2} and that the interfacial shear stress was

$$\tau_1 = \mu(P_0 + P_a) \quad (2)$$

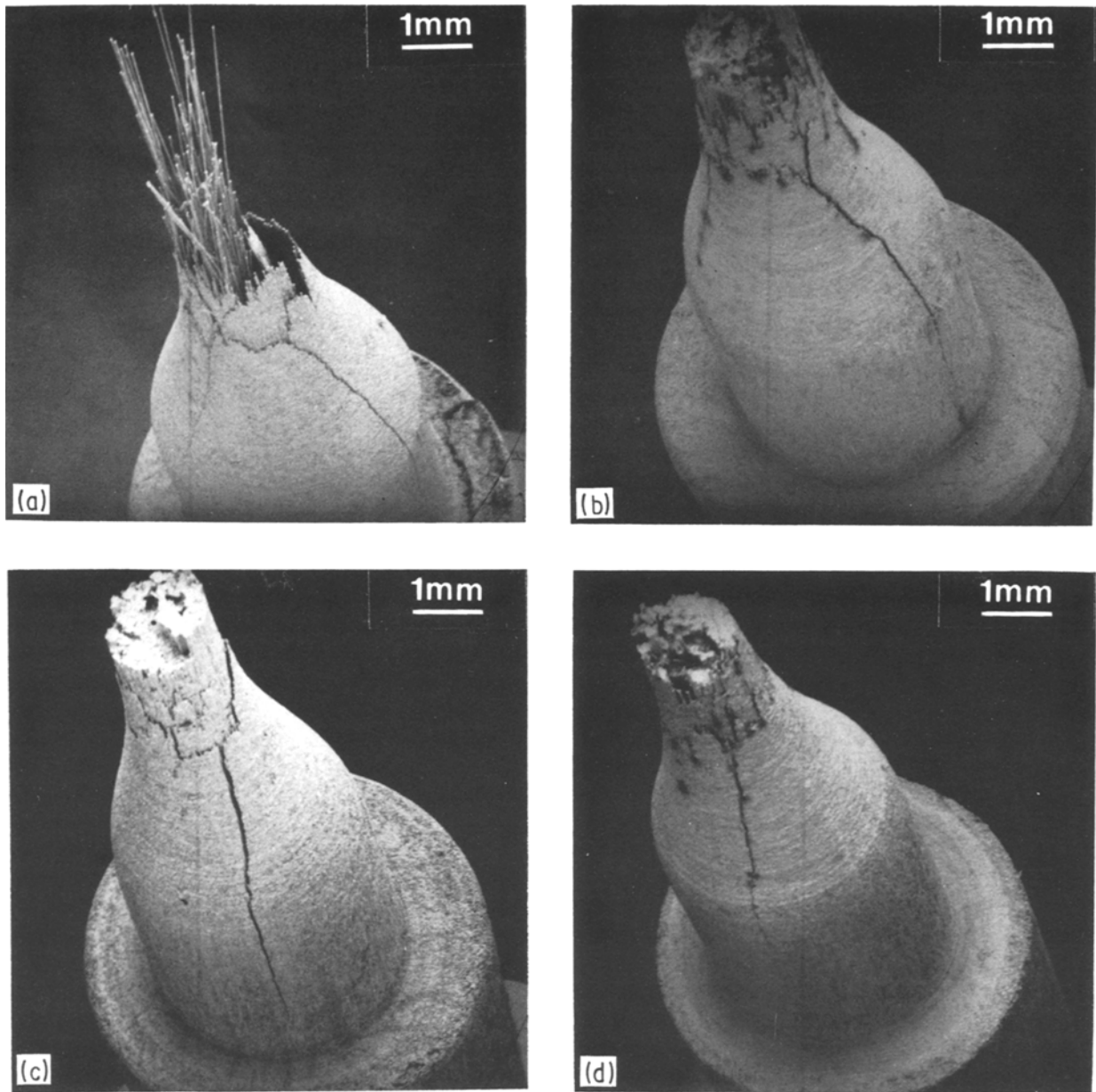


Figure 2 Scanning electron fractographs of pultruded GRP specimens tested in tension (a) at atmospheric and under superposed hydrostatic pressures of (b) 100, (c) 250 and (d) 350 MN m^{-2} . Note the persistence of cracks at higher pressures.

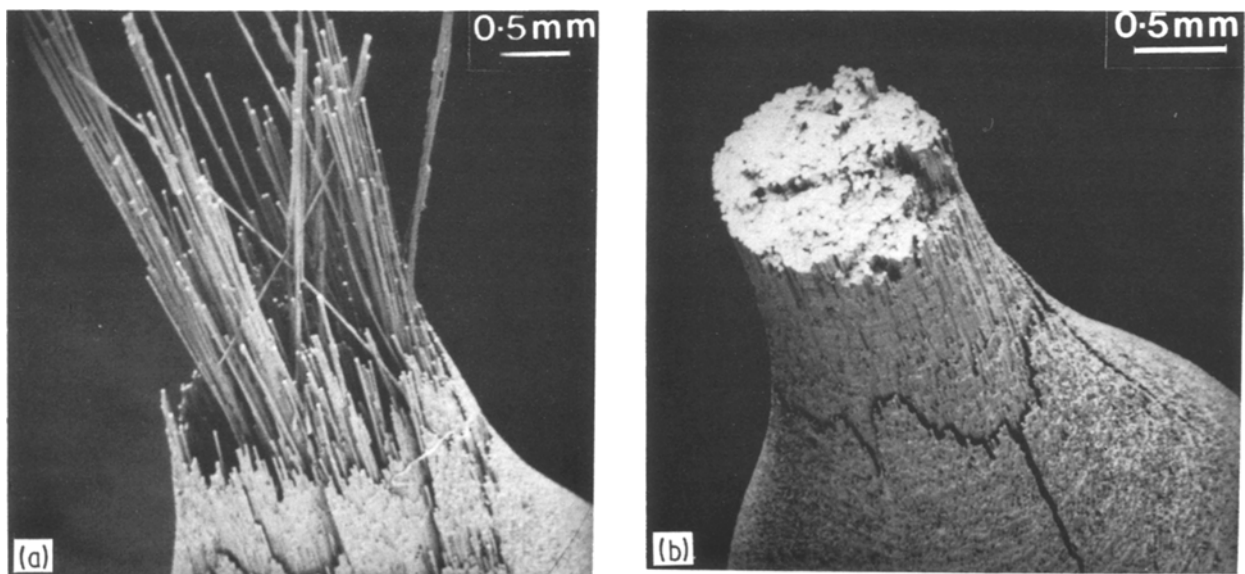


Figure 3 Scanning electron fractograph, at higher magnifications than in Fig. 2, showing in detail (a) the random bundle type of pull-out at atmospheric pressure and (b) the reduced fibre pull-out at 300 MN m^{-2} , producing the fairly flat fracture, but also the persistence of cracking (absent in CFRP at comparable pressures).

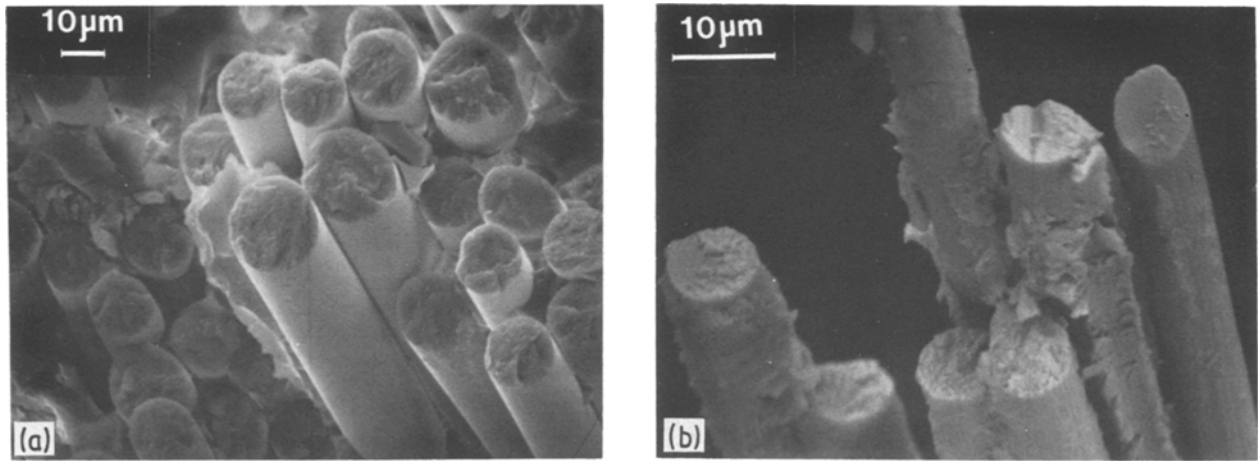


Figure 4 Tensile failures of (a) GRP at 300 MN m^{-2} and (b) CFRP at atmospheric pressure showing clearly resin adhering to the carbon fibres and “clean” pulled-out glass fibres.

where P_0 was the shrinkage pressure, P_a was the externally applied pressure (up to 10 MN m^{-2}) and μ was in the range 0.18 to 2.4. Their relatively high experimental scatter, however (see their Fig. 9), is to be noted. Earlier Bowden [22], working with steel/epoxy in the pressure range extending to 70 MN m^{-2} , showed the shear strength of the adhesive bond to be marginally lower than the resin yield strength, but also reported an indication that its pressure dependence is higher. The shrinkage stress was calculated as 7 MN m^{-2} (three times lower than Chua and Piggott’s [19] value) and atmospheric friction stress as 3 MN m^{-2} , rising to 22 MN m^{-2} at 65 MN m^{-2} applied pressure.

It is not clear if any of these values and pressure dependences relate to the debonding of fibre bundles; Chua and Piggott [18–20] have concluded that the interface behaves in a very complex fashion and the (single) fibre pull-out process is governed by at least five factors. As our glass fibres were “clean” in the entire testing pressure range, five times that of Bowden and 35 times that of Chua and Piggott, we concluded that direct measurement of σ_a and its pressure dependence in our material was necessary.

Using 3 mm thick discs cut from the composite rod we investigated the behaviour in diametral compression [23, 24], i.e. using a testing technique for the measurement of tensile strength of brittle materials, especially rocks. (Details of these biaxial stressing experiments will be presented elsewhere). The tensile strength (under transverse compression) was evaluated as

$$\sigma_d = \frac{2F}{\pi Dt} \quad (3)$$

noting that the associated transverse compression stress is three times this value, where F is the compressive load and D and t are the specimen diameter and thickness, respectively. Fractures were clean, emanating from the centre and along the loading axis diameter. σ_d was thus identified as the debonding stress, σ_a . The atmospheric biaxial value of σ_d , 69 MN m^{-2} , was interpreted to correspond to a (uniaxial) debonding stress of $\sim 52 \text{ MN m}^{-2}$ and the pressure dependence to be ~ 0.12 per 100 MN m^{-2}

superposed pressure. The value of σ_d , 52 MN m^{-2} , is not inconsistent with Chua and Piggott’s [18] estimate of the maximum interfacial shear stress of 21 to 34 MN m^{-2} and our pressure dependence is within their (large) scatter band for τ_i [19].

Taking the bundle diameter D to be 0.4 mm, and σ_a to be 52 MN m^{-2} , Equation 1 evaluates R to be 5.7 mm, consistent with observed bundle curvatures. As the critical stress at the limit of proportionality (Fig. 1) increased from 0.95 at atmospheric to 1.25 GN m^{-2} at 300 MN m^{-2} superposed pressure, ~ 0.09 per 100 MN m^{-2} superposed pressure, σ_a increased by ~ 0.12 per 100 MN m^{-2} superposed pressure. This agreement is considered good enough to account for the pressure dependence of σ_c , only some 35% of the relevant value of the slope for CFRP, in which the associated mechanism was interpreted to be resin yielding.

In compression, in this GRP, bundle curvature was postulated to increase, and matrix yielding rather than decohesion to control debonding initiation and also failure, bundle buckling being easy due to the relatively low value of E for GRP [9]. In tension the bundle curvature is decreased and final failure is by breaking of the fibres, initially bundles at various cross-sections, but ultimately in nearly a specific cross-section (e.g. Fig. 2c). Only then, $H > 300 \text{ MN m}^{-2}$ superposed pressure, was the ultimate load-carrying capacity of the rod controlled by fibre strength; accordingly σ_t appears independent of pressure above 300 MN m^{-2} . At lower pressures, delamination occurred as the load was increasing; the straightening of detached, initially curved surface bundles, it is suggested, enabled additional loads to be carried until numerous fibre failures took place. Superposition of transverse (part of the hydrostatic) pressure made interlaminar cracking more difficult and therefore also the enhanced load transfer. Thus failure strength decreased with increasing pressure (Fig. 1). This interpretation follows closely that proposed for CFRP [10] and, as for that material, we would suggest that only for the lower bound of composite strength (flat fractures) are the statistical theories (at a given cross-section) of composite failure relevant.

The results indicate that for axial tension of GRP, fibre bundle curvature and interfacial properties are pertinent, whereas in axial compression bundle curvature and resin strength are relevant. Only when stress redistribution between fibre bundles is suppressed (i.e. at 350 MN m^{-2}) was the tensile behaviour of our GRP solely governed by the strength properties of the fibres.

Acknowledgement

The authors wish to acknowledge the support of the Science and Engineering Research Council.

References

1. M. FUWA, A. R. BUNSELL and B. HARRIS, *J. Mater. Sci.* **10** (1975) 2062.
2. M. FUWA, B. HARRIS and A. R. BUNSELL, *J. Phys. D.* **8** (1975) 1460.
3. A. R. BUNSELL and D. VALENTIN, *Compos. Struct.* **1** (1983) 67.
4. C. ZWEBEN and B. W. ROSEN, *J. Mech. Phys. Solids* **18** (1970) 189.
5. D. G. HARLOW and S. L. PHOENIX, *J. Compos. Mater.* **12** (1978) 195.
6. B. W. ROSEN, *Amer. Inst. Aeronaut. Astronaut. J.* **2** (1964) 1985.
7. T. V. PARRY and A. S. WRONSKI, *J. Mater. Sci.* **16** (1981) 439.
8. *Idem, ibid.* **17** (1982) 893.
9. A. S. WRONSKI and T. V. PARRY, *ibid.* **17** (1982) 3656.
10. *Idem, ibid.* **19** (1984) 3421.
11. T. V. PARRY and A. S. WRONSKI, *ibid.* **20** (1985) 2141.
12. P. D. EWINS and R. T. POTTER, *Phil. Trans. R. Soc.* **A2294** (1980) 507.
13. A. S. WRONSKI and M. PICK, *J. Mater. Sci.* **12** (1977) 28.
14. A. S. WRONSKI and T. V. PARRY, in Proceedings of 1st International Conference on Post Failure Analysis: Techniques for Fiber Reinforced Composites, Dayton, Ohio, July 1985, edited by F. Feчек (Air Force Wright Aeronautical Laboratories) p. 2-1.
15. E. WILKINSON, T. V. PARRY and A. S. WRONSKI, *Compos. Sci. Technol.* **23** (1986) 17.
16. M. R. PIGGOTT, *J. Mater. Sci.* **16** (1981) 2837.
17. D. G. SWIFT, *J. Phys. D., Appl. Phys.* **8** (1975) 223.
18. P. S. CHUA and M. R. PIGGOTT, *Compos. Sci. Technol.* **22** (1985) 33.
19. *Idem, ibid.* **22** (1985) 107.
20. *Idem, ibid.* **22** (1985) 185.
21. M. R. PIGGOTT and P. S. CHUA, *Ind. Eng. Chem. — Product R/D* in press.
22. P. B. BOWDEN, *J. Mater. Sci.* **5** (1970) 517.
23. G. HONDROS, *Austral. J. Appl. Sci.* **10** (1959) 243.
24. R. BERENBAUM and I. BRODIE, *Br. J. Appl. Phys.* **10** (1959) 281.

Received 24 February
and accepted 28 April 1986